

Comparison between Measured Scrape-off Layer Plasma Parameters and 2-D Model Calculations for JET X-point Discharges

A Loarte, A Chankin, S Clement, G Corrigan, P Harbour,
L Horton, G Janeschitz¹, J Lingertat, G Matthews, R Simonini,
J A Tagle², A Taroni, G Vlases.

JET Joint Undertaking, Abingdon, Oxon, OX14 3EA.

¹ ITER-EDA, Garching, Germany.

² IBERDROLA, Madrid, Spain.

"This document is intended for publication in the open literature. It is made available on the understanding that it may not be further circulated and extracts may not be published prior to publication of the original, without the consent of the Publications Officer, JET Joint Undertaking, Abingdon, Oxon, OX14 3EA, UK".

"Enquiries about Copyright and reproduction should be addressed to the Publications Officer, JET Joint Undertaking, Abingdon, Oxon, OX14 3EA".

1. INTRODUCTION.

Two dimensional fluid codes for the plasma linked with a Monte-Carlo (or diffusive) code for the neutrals [1,2,3] are routinely used to predict the performance of divertor tokamak experiments and reactors. Hence, it is necessary to compare the predictions of these codes with experimental measurements in order to assess the reliability of the models and assumptions contained in them. Such a study is presented in this paper for the JET 2-D fluid code EDGE2D/U [1] using experimental measurements from JET diverted discharges.

2. EXPERIMENTAL MEASUREMENTS.

The basic measurements used in this assessment are from Langmuir probes embedded in the divertor target plate and from a reciprocating Langmuir probe which enters the scrape-off layer plasma away from the divertor region. Bolometric measurements for the main plasma and divertor region are also used to determine (together with the input power and diamagnetic energy) the energy flow out of the main plasma to the SOL. Generally, the main uncertainties involved in the Langmuir probe measurements are those associated with their effective area, which determines the value of the electron density measured, and with the position of the probe with respect to the magnetic separatrix. The location of the target probes with respect to the magnetic separatrix is determined very accurately [4]. However, the effective area of these probes may be affected by shadowing from parts of the divertor plate and may change due to erosion during the course of the experiments. On the other hand, the reciprocating effective area is well defined, whereas its position with respect to the magnetic separatrix is determined with a typical accuracy of 1 cm at the outer midplane [5]. Since the

typical fall off length of plasma parameters in the SOL is of the order of 1 cm or less, it is clear that the relative position of the probe to the separatrix must be known with a much higher accuracy in order to assess quantitatively the gradients of the SOL plasma parameters along the field lines. For this reason, in our study we use the conservation of electron pressure along the field lines (no large momentum losses), which connect the reciprocating probe and the target probes, to determine the distance between the reciprocating probe and the separatrix [6]. In this paper we consider discharges in all confinement regimes (Ohmic, L-mode, H-mode) and in deuterium and hydrogen.

3. MODELLING ASSUMPTIONS AND INPUTS.

3.1. MODELLING ASSUMPTIONS.

The code EDGE2D/U contains physical models with various degrees of sophistication; in this study we have used the code in the simplest way to model basic features of the discharges and leave the investigation of more complicated experimental features with more advanced models to the future. Hence, only modelling of pure plasmas has been carried out and no drift terms have been included nor has the influence of currents in the SOL on the sheath boundary conditions been considered. The only asymmetries between the divertor strike zones contained in the model are those associated with the toroidal geometry of the SOL and no other intrinsic term that may lead to such asymmetries, such as momentum transfer from the main plasma to the SOL [7], has been included. Correspondingly, only measurements at the outer divertor target are presented in this study.

The real non orthogonal geometry of the divertor target has been used in the modelling and perfect recycling (recycling coefficient $R = 1$) assumed (a sensitivity study performed is discussed in section 4.3).

Transport is assumed to be classical along the field line and anomalous across the field. Only a flux limit for the momentum flux along the field is used [8], which is important to avoid unphysically large viscous effects at high SOL temperatures. Two basic assumptions can be used in the code to characterize the radial anomalous transport which determine the value of the radial diffusion coefficients

deduced from modelling the experiment : either the radial fluxes are driven by gradients of temperature and density in the radial coordinate or they are driven by gradients in magnetic flux coordinate. In the first case the diffusion coefficients are poloidally constant (in our notation D_{\perp} , χ_{\perp}), in the second case they increase with poloidal flux expansion (\hat{D}_{\perp} , $\hat{\chi}_{\perp}$ will represent their value at the outer midplane).

One of the problems found in modelling most of the discharges in JET is that the region over which the field lines connect both divertor strike zones without intersecting any other material surface (i.e. "pure single-null" configuration) is relatively narrow, typically $\lesssim 2$ cm at the outer midplane, which is comparable to the typical SOL thickness. Hence the radial boundary conditions at the outer edge of the SOL must be defined consistently with the diffusion coefficients used in the modelling. This is done by imposing a decay length in the outer edge of the SOL, deduced from the calculated profiles with the assumption that the density profiles decay exponentially from the separatrix and the temperature profiles follow approximately the dependence obtained if conduction along the field dominates i.e. $T \propto (Const. + \Delta R)^{-4/5}$ [9]. Other typical assumptions, valid when the "magnetic SOL" is very broad, such as assuming given small values of plasma parameters in the outer part of the computational domain or zero gradients there, are obviously not applicable in our case.

3.2. MODEL INPUTS VARIED TO FIT EXPERIMENTAL DIVERTOR PARAMETERS.

The basic inputs which determine the SOL plasma parameters in EDGE2D/U are the total hydrogenic ion content in the computational domain and the power flow out of the main plasma carried by the electrons and the ions into this domain. These two inputs together with the effective transport coefficients for anomalous transport determine the main SOL plasma density and temperature profiles. In JET, measurements of the ion temperature at the plasma edge are very sparse, hence we usually assume that the same power flows out of the main plasma the SOL via the electrons and the ions.

The experimental situation with respect to the power balance is unclear in JET discharges. From Langmuir probe measurements, the power balance is

satisfactory for Ohmic and low power L-mode discharges. For high power L-modes and H-modes the situation is unsatisfactory because although the probes clearly show a worsening of the power balance [10], there are indications from infrared measurements which point towards a similar power balance in L-mode and H-mode [11]. This was attributed in [11] to the proximity between the X-point and the divertor plate for those discharges, which favours a better estimate (with infrared measurements) of the recycling losses deposited onto the target. Another possible explanation for this disagreement is based on the large electron currents observed in JET close to the separatrix strike point [12] and which have not been considered to calculate the power measured with the Langmuir probes. In principle, the power flow associated with these currents could be of the same order of magnitude of the missing power, but its estimate depends critically on the influence of secondary electron emission on the sheath transmission coefficient, which is poorly known. Hence, these measurements close to the separatrix strike point are not considered in the study performed in this paper, where we assume that their influence in the plasma parameters away from the strike point is negligible.

Despite the experimental uncertainties, the power which enters the SOL to be used in the code cannot be much larger than that determined experimentally from bulk plasma measurements (because of different asymmetries in code and experiment, and modelling only performed for the outer divertor). Hence, in the modelling, the power which enters the SOL via the electrons and ions channels $P_{e,i}$ must satisfy

$$P_e + P_i \lesssim P_{SOL} = P_{INP} - P_{RAD}^{BULK} - \dot{W} \quad (1)$$

where P_{INP} is the input power, P_{RAD}^{BULK} is the power radiated in the bulk plasma and \dot{W} is the time derivative of the plasma diamagnetic energy. However, due to the different asymmetries in the code and the experiment only trends in the power balance for various regimes can be assessed from the comparison of modelling and experiment. The values of D_{\perp} , χ_{\perp} used in modelling are determined from the measured plasma parameter profiles in the main SOL and at the divertor target.

4. DISCHARGES MODELLED AND MODELLING RESULTS.

4.1. DISCHARGES WITH ONLY DIVERTOR TARGET MEASUREMENTS.

The parameters for a series of hydrogen discharges using the upper JET divertor target (Carbon target) in various confinement regimes which has been modelled are given in Table 1 (Δ_x is the distance between X-point and divertor target).

Pulse	Conf.	I (MA)	B_ϕ (T)	Δ_x (cm)	$\langle n_e \rangle$ ($10^{19} m^{-3}$)	P_{INP} (MW)	P_{SOL} (MW)	P_{RAD}^{DIV} (MW)
24165	Ω	3	3.2	9.6	1.2	1.6	1.2	0.2
24175	L	3	2.1	8.9	1.1	5.5	4.9	0.4
24171	H	3	2.1	7.9	2.3	8.0	4.2	0.3

Table 1. Plasma parameters for the hydrogen discharges modelled.

The summary of the modelling results for these discharges is given in table 2.

Pulse	n_{sep} ($10^{18} m^{-3}$)	$\frac{n_{sep}}{\langle n_e \rangle}$ (%)	$P_e = P_i$ (MW)	$\frac{(P_e + P_i)}{P_{SOL}}$ (%)	\hat{D}_\perp (m^2/s)	$\hat{\chi}_{1e,i}$ (m^2/s)
24165	5.3	44	0.7	87	0.1	0.5
24175	5.2	46	1.6	65	0.2	0.5
24171	6.5	28	0.8	38	0.05	0.25

Table 2. Modelling results for discharges in Table 1.

An example of the temperature profiles obtained with EDGE2D/U and from probe measurements at the divertor target for the ohmic discharge is shown in Fig. 1. By mapping these profiles along the field lines it is possible to represent midplane SOL profiles and target profiles versus flux surface spacing at a given spatial position. In the following figures this has been done taking as reference spatial point the outer midplane of JET. In Fig.2 the mapped profiles for the ohmic discharge are shown.

The effective values of the diffusion coefficients to be used in order to model the measurements are very small (particularly \hat{D}_\perp) as reported in [13], which is in agreement with similar results for DIII-D [14] and ASDEX-Upgrade [15]. They

are much smaller than the Bohm value which, for instance, for the discharge 24165 would be $D_{\perp}^{Bohm} \simeq 1 \text{ m}^2/\text{s}$). The values of the deduced transport coefficients follow the trend expected from the changes in main plasma confinement, being larger for L-mode than for H-mode.

The trends in the power balance with Langmuir probes for various confinement regimes are also reflected in the modelling of these discharges. However the percentage of power into the SOL (compared to P_{SOL}) used in the simulations is higher than that deduced from the experimental interpretation of the Langmuir probe measurements, where electron and ion temperatures are assumed to be equal. This is due mainly to the behaviour of the calculated ion temperature which tends to be higher than the electron temperature and has a much flatter profile (both factors increase the amount of power that arrives at the divertor target for the same electron parameters). Although for these discharges no measurements were available for the main SOL plasma parameters, the values of separatrix density used in the model are consistent with those from similar discharges from the JET/DIII-D database [16], in particular the drop in the ratio of separatrix to main plasma densities when the discharges are in the H-mode.

As these pulses do not show very high recycling at the divertor (low n_{sep}), the energy coupling between electrons and ions in the SOL is very weak and hence it is possible to obtain similar results for the electron parameters (n_e , T_e) with much higher ion temperatures (taking $P_i \gg P_e$) and much better power balance correspondingly. This study has been done for the pulse 24171 whose electron SOL and divertor parameters can be obtained with the same transport coefficients and taking $P_e = 0.7 \text{ MW}$ and $P_i = 3.0 \text{ MW}$.

4.2. DISCHARGES WITH MEASUREMENTS AT DIVERTOR TARGET AND MAIN SOL.

The parameters for two deuterium discharges using the lower JET divertor target (Beryllium target) in L-mode which have been modelled are given in table 3. For these discharges measurements are available both in the main SOL and the divertor target.

Pulse	Conf.	I (MA)	B_ϕ (T)	Δ_x (cm)	$\langle n_e \rangle$ ($10^{19} m^{-3}$)	P_{INP} (MW)	P_{SOL} (MW)	P_{RAD}^{DIV} (MW)
25720	L	3	2.9	8.0	1.6	3.2	2.4 (*)	0.7 (*)
25710	L	3	2.9	8.0	2.6	3.4	2.7 (*)	1.9 (*)

(*) The divertor radiation is somewhat uncertain for JET Beryllium target X-point discharges because of restrictions in the field of view of the bolometer cameras.

Table 3. Plasma parameters for the deuterium discharges modelled.

The summary of the modelling results for these discharges is given in table 4.

Pulse	n_{sep} ($10^{18} m^{-3}$)	$\frac{n_{sep}}{\langle n_e \rangle}$ (%)	$P_e = P_i$ (MW)	$\frac{(P_e + P_i)}{P_{SOL}}$ (%)	\hat{D}_\perp (m^2/s)	$\hat{\chi}_{1e,i}$ (m^2/s)
25720	5.5	34	0.7	58	0.05	0.7
25710	9.2	35	1.1	81	0.05	0.5

Table 4. Modelling results for discharges in Table 3.

The comparison between the results of these calculations and the measurements is shown in Fig.3 for discharge 25720 and Fig. 4 for discharge 25710. Due to the uncertainty in the distance between the reciprocating probe and the separatrix, the profiles measured with this probe have been shifted so as to obtain experimental electron pressure balance. The agreement between experiment and model is good for the low density pulse (25720) and slightly worse for the high density one (25710). This trend holds at higher densities and it is due to the absence of impurity radiation in our model which becomes dominant at higher densities for these levels of input power. Another trend which is observed when comparing hydrogen and deuterium discharges is that the particle diffusion coefficients tend to be smaller for deuterium as seen in the ratio of separatrix density to line average density used in the modelling. This is associated with a higher ionization in the divertor for the case of deuterium.

4.3. SENSITIVITY STUDIES.

Some sensitivity studies have been performed in order to assess the dependence of the results on the assumptions made in modelling :

- Radial Transport : Similar results in the main SOL and the divertor target can be obtained for either assumption (radial fluxes proportional to spatial gradients or gradients in magnetic flux) provided that the values of the transport coefficients are taken as

$$D_{\perp} \text{ (Radial spacing)} \simeq 2 \times \hat{D}_{\perp} \text{ (Magnetic Flux spacing)}. \quad (2)$$

The same relation holds for χ_{\perp} . Very different plasma parameters and decay lengths in the private flux region are found for either case (steeper for radial spacing). The existing measurements in the private flux region of the JET divertor fall in between the two assumptions being more consistent with magnetic flux spacing driven fluxes, but the spatial resolution of the measurements is too coarse to draw definite conclusions. The asymmetry for the power arriving at the divertor strike zones calculated with the code is associated with the toroidal geometry of the SOL and the Shafranov shift which compresses the flux surfaces in the outer side of the torus. This asymmetry depends on the transport model and increases with plasma collisionality, being larger (5 - 15 %, for the discharges modelled) for radial spacing driven fluxes. However, the typical power asymmetry value calculated (30% more power to the outer side) may be very different from that found in experiment which depends on discharge conditions [17].

- Recycling coefficient : At low divertor densities the relation between the midplane and divertor scrape-off layer densities depends weakly on the value of the recycling coefficient used (provided $R \simeq 1$). However, at higher densities the value of the calculated divertor density (for the same midplane density) is more sensitive to the value of R assumed. For instance, in modelling the discharge 25710, it was found that reducing the recycling coefficient to 0.95 decreased the divertor density by approximately 40% for the same midplane density. Hence, an experimental assessment of the value of the recycling coefficient is needed in order to model accurately high density discharges.

5. CONCLUSIONS AND FURTHER WORK.

Measured plasma parameters at the divertor target of JET can be modelled for all regimes with reasonable or "measured" (once corrected for electron pressure balance) main SOL plasma parameters. While the modelled power balance is

satisfactory in ohmic and L-mode discharges a sizeable amount of power cannot be accounted for (assuming $P_e \simeq P_i$) in H-mode discharges. Very small values of the effective diffusion coefficients (one to two orders of magnitude smaller than Bohm, for particle diffusion) must be used to match the measured steep radial profiles of electron density and temperature. The modelled and measured main SOL plasma density profiles decay exponentially from separatrix while temperature profiles do not decay exponentially because of the contribution of conduction to the energy transport along the field. Modelling of the discharges with full impurity treatment has been performed and the preliminary results are encouraging but further work in this line is needed to assess the transport of impurities in divertor discharges.

Acknowledgments : J. Spence is acknowledged for his technical assistance in the use of EDGE2D/U.

6. REFERENCES.

- [1] Simonini, R., Corrigan, G., Radford, G., et al., *Contrib. Plasma Phys.* **34** (1994) 368.
- [2] Schneider, R., Reiter, D., Zehrfeld, H.P., et al., *J. Nucl. Mater.* **196 - 198** (1992) 810.
- [3] Rognlén, T.D., Milovich, J.L., Rensink, M.E., et al., *J. Nucl. Mater.* **196 - 198** (1992) 347.
- [4] O'Brien, D.P.J., Ellis, J.J., Lingertat, J., *Nucl. Fusion* **33** (1993) 467.
- [5] Zwingmann, W., Ellis, J.J., Lingertat, J., et al., *Proc. 20th EPS Conf. Contr. Fus. & Plasma Phys.*, Vol. 17C Part I (1993) 195.
- [6] Vlases, A., JET Team, *Proc. 14th IAEA Conf. Plasma Phys. & Contr. Nucl. Fusion Res.*, Vol. 1 (1992) 287.
- [7] Chankin, A., et al., 11th PSI Conference, Mito, Japan (1994).
- [8] Radford, G., *Contrib. Plasma Phys.* **32**(1992) 297.
- [9] Keilhacker, M., Lackner, K., Behringer, K., et al., *Physica Scripta*. **T2/2** (1982) 443.
- [10] Loarte, A., PhD Thesis, Universidad Complutense de Madrid (1992).
- [11] Chankin, A., Summers, D.D.R., Jaekel, H.J., et al., *Plasma Phys. and Contr. Fusion* **36** (1994) 403.
- [12] Lingertat, J., et al., 11th PSI Conference, Mito, Japan (1994).
- [13] Simonini, R., Taroni, A., Keilhacker, M., et al., *J. Nucl. Mater.* **196 - 198** (1992) 369.
- [14] Porter, G.D, ITER Tech. Meet. & Workshop on Divertor Physics Garching (FRG) 1994.
- [15] Bosch, H.S., Schneider, R., Pitcher, C.S., et al., *Proc. 20th EPS Conf. Contr. Fus. & Plasma Phys.* Vol. 17C Part II (1993) 795.
- [16] Matthews, G.F., Jong, R.A., Porter, G.D., et al., 35th APS Div. Plasma Phys. Meet., St Louis (USA) 1993.
- [17] Reichle, R., Clement, S., Gottardi, N., et al., *Proc. 18th EPS Conf. Contr. & Plasma Phys.*, Vol. 15C Part III (1991) 105.

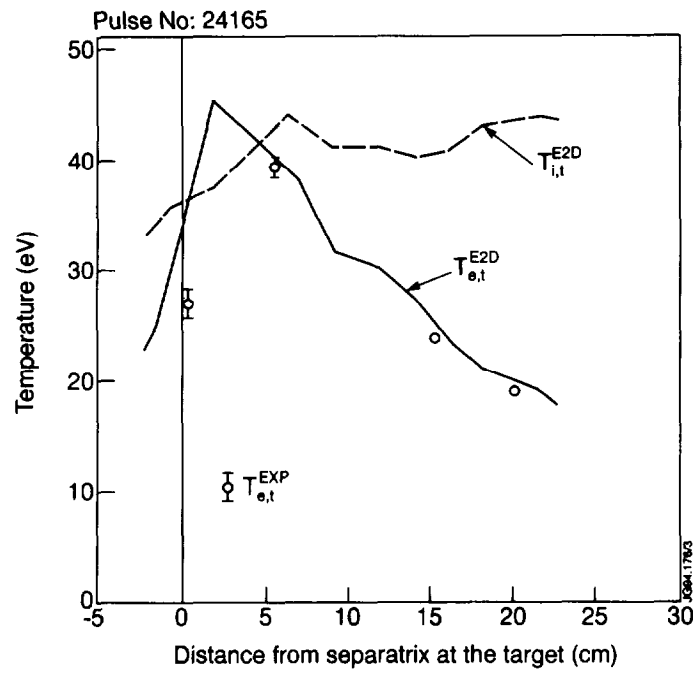


Fig.1. Measured Electron Temperature at the divertor target (EXP) and modelled (E2D) Electron and Ion Temperatures.

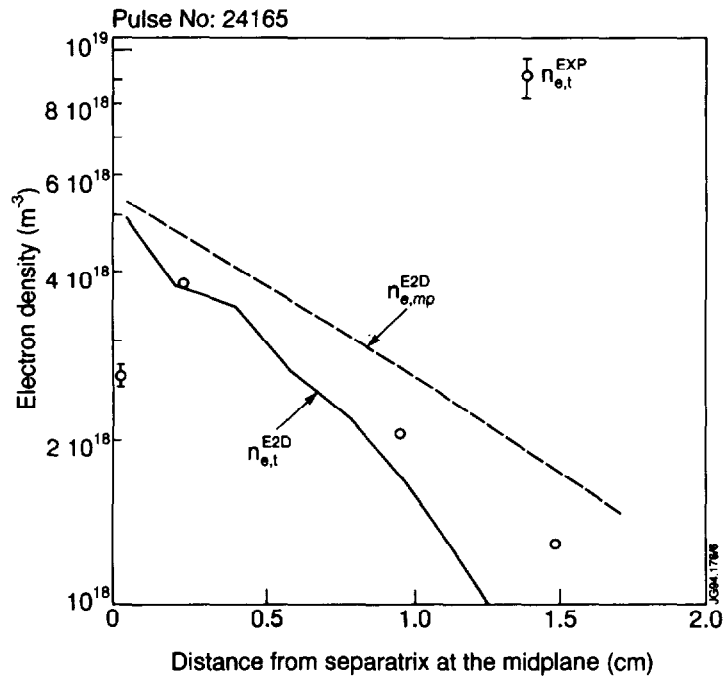
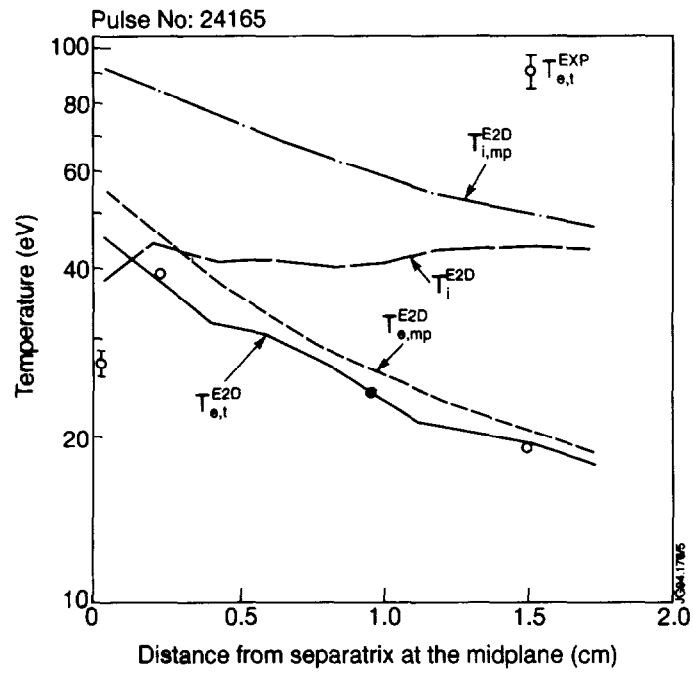


Fig.2. (a) Measured Electron Temperature at the divertor target (EXP) and modelled (E2D) Electron and Ion Temperatures at the midplane (mp) and divertor target (t). (b) Measured Electron Density ($T_i \simeq T_e$ assumed) at the divertor target (EXP) and modelled (E2D) Electron Density at the midplane (mp) and divertor target (t). The divertor target profiles are mapped to the outer midplane along the flux surfaces.

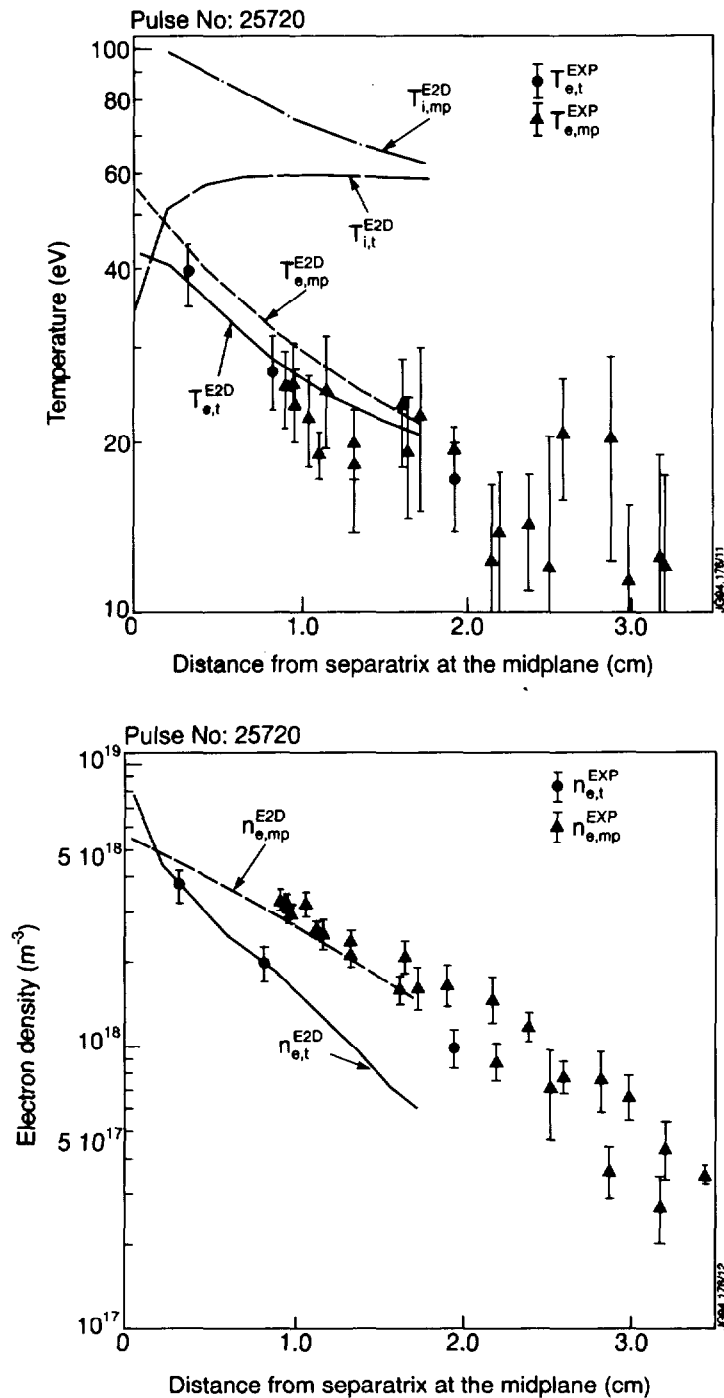


Fig.3. (a) Measured Electron Temperature (EXP) at the divertor target (t) and the midplane (mp) and modelled (E2D) Electron and Ion Temperatures at the midplane (mp) and divertor target (t). (b) Measured Electron Density ($T_i \simeq T_e$ assumed) (EXP) at the divertor target (t) and the midplane (mp) and modelled (E2D) Electron Density at the midplane (mp) and divertor target (t). The divertor target profiles are mapped to the outer midplane along the flux surfaces. The midplane profiles are shifted with respect to the calculated magnetic separatrix so as to achieve experimental electron pressure balance.

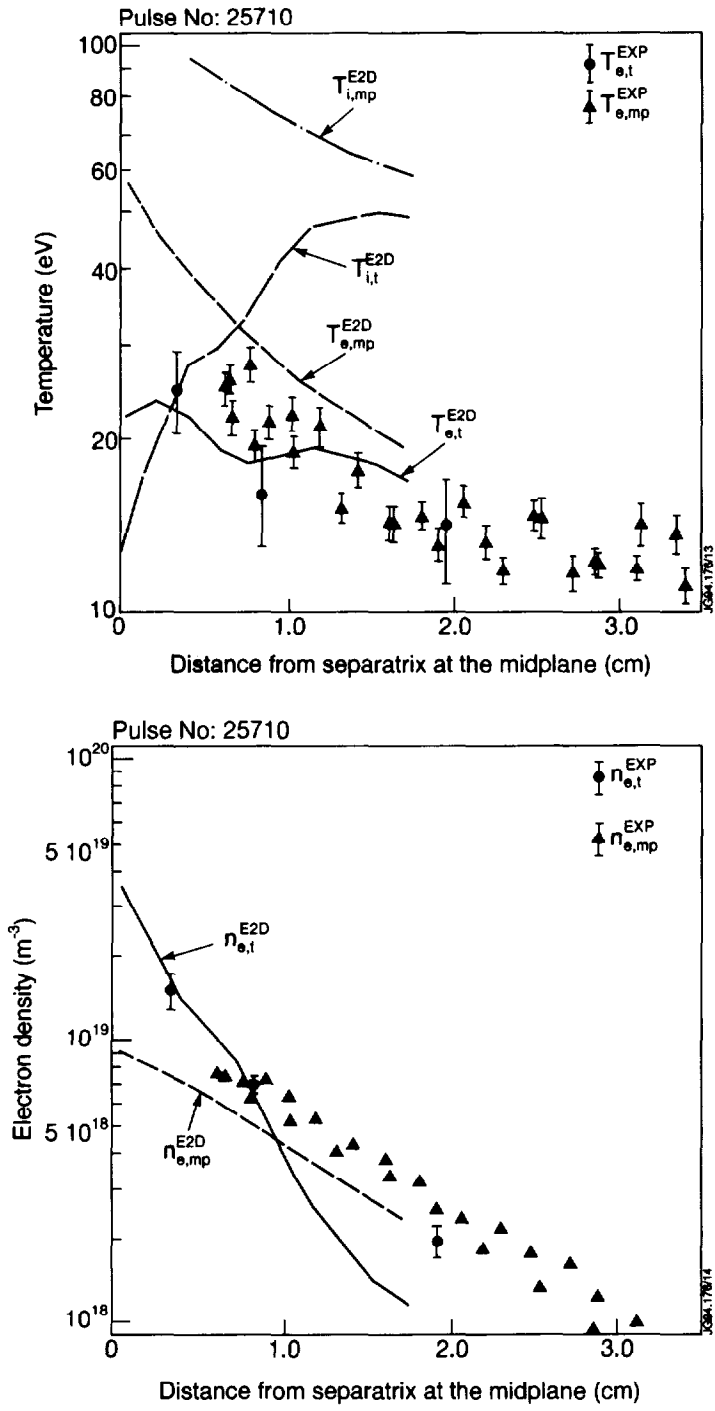


Fig.4. (a) Measured Electron Temperature (EXP) at the divertor target (t) and the midplane (mp) and modelled (E2D) Electron and Ion Temperatures at the midplane (mp) and divertor target (t). (b) Measured Electron Density ($T_i \simeq T_e$ assumed) (EXP) at the divertor target (t) and the midplane (mp) and modelled (E2D) Electron Density at the midplane (mp) and divertor target (t). The divertor target profiles are mapped to the outer midplane along the flux surfaces. The midplane profiles are shifted with respect to the calculated magnetic separatrix so as to achieve experimental electron pressure balance.